Cell, Vol. 109, 87–99, April 5, 2002, Copyright ©2002 by Cell Press

Expansion of the Cell Plate in Plant Cytokinesis Requires a Kinesin-like Protein/MAPKKK Complex

Ryuichi Nishihama,[1,4] Takashi Soyano,[1] Masaki Ishikawa,[1] Satoshi Araki,[1,6] Hirokazu Tanaka,[1] Tetsuhiro Asada,[2] Kenji Irie,[1] Mayumi Ito,[1] Mizuya Terada,[1] Hiroharu Banno,[1,5] Yoshiko Yamazaki,[1] and Yasunori Machida[1,3]

[1]Division of Biological Science
Graduate School of Science
Nagoya University
Chikusa-ku, Nagoya 464-8602
Japan

[2]Department of Biology
Graduate School of Science
Osaka University
Toyonaka 560-0043
Japan

Summary

The tobacco mitogen-activated protein kinase kinase kinase NPK1 regulates lateral expansion of the cell plate at cytokinesis. Here, we show that the kinesin-like proteins NACK1 and NACK2 act as activators of NPK1. Biochemical analysis suggests that direct binding of NACK1 to NPK1 stimulates kinase activity. NACK1 is accumulated specifically in M phase and colocalized with NPK1 at the phragmoplast equator. Overexpression of a truncated NACK1 protein that lacks the motor domain disrupts NPK1 concentration at the phragmoplast equator and cell plate formation. Incomplete cytokinesis is also observed when expression of *NACK1* and *NACK2* is repressed by virus-induced gene silencing and in embryonic cells from *Arabidopsis* mutants in which a *NACK1* ortholog is disrupted. Thus, we conclude that expansion of the cell plate requires NACK1/2 to regulate the activity and localization of NPK1.

Introduction

Cell division in eukaryotes culminates in cytokinesis, with appropriate distribution of nuclear and cytoplasmic genetic information to daughter cells. Cell division in animals and plants appears quite dissimilar: animal cells divide by constriction of the cell cortex, whereas plant cells divide by formation of new cross walls, known as cell plates, from the center to the periphery of each dividing cell (Field et al., 1999).

In plant cytokinesis, formation of the cell plate occurs in the phragmoplast, a complex structure composed mainly of microtubules (MTs) and microfilaments (reviewed in Staehelin and Hepler, 1996; Heese et al., 1998; Nishihama and Machida, 2001). At late anaphase, a phragmoplast appears midway between two daughter nuclei, with two antiparallel bundles of MTs being aligned such that the plus ends of the MTs overlap (Gunning, 1982). Golgi-derived membranous vesicles carrying cell plate materials are then transported to the equatorial zone of the phragmoplast where they fuse to create a membranous network, which matures into a cell plate (Samuels et al., 1995). The continuous outward redistribution of MTs transforms the phragmoplast into a ring and increases its diameter, allowing the cell plate to expand laterally until it reaches the cell wall (Yasuhara et al., 1993; Yasuhara and Shibaoka, 2000). The KNOLLE syntaxin homolog, the KEULE Sec1 homolog, and the KORRIGAN cellulase are essential for such plant cytokinesis (Lukowitz et al., 1996; Zuo et al., 2000; Assaad et al., 2001).

Proteins related to vesicle trafficking and MT-associated proteins, including kinesin-like motor proteins (KLPs), are concentrated at the phragmoplast (Lloyd and Hussey, 2001; Nishihama and Machida, 2001; Lee et al., 2001). Protein kinases, such as mitogen-activated protein kinases (MAPKs), $p43^{Ntf6}$ in tobacco (Calderini et al., 1998), and MMK3 in alfalfa (Bögre et al., 1999), accumulate at the cell plate, while NPK1 (*n*ucleus- and *p*hragmoplast-localized protein *k*inase 1) MAPK kinase kinase (MAPKKK) accumulates in the equatorial region of the tobacco phragmoplast (Nishihama et al., 2001). Activation of these kinases at late M phase (Calderini et al., 1998; Bögre et al., 1999; Nishihama et al., 2001) suggests the involvement of the coordinated actions of these enzymes in formation of the cell plate. This hypothesis is supported by the observation that overexpression of a kinase-negative form of NPK1 in tobacco cells inhibits expansion of both the phragmoplast and the cell plate, with resultant generation of multinucleate cells with incomplete cell plates (Nishihama et al., 2001).

It has been suggested that the noncatalytic region of NPK1 might be involved in activation of this MAPKKK (Banno et al., 1993; Nishihama et al., 1997). Expression of NPK1 or its *Arabidopsis* ortholog, ANP1, can suppress mutations in genes for MAPKKKs in yeast. Removal of noncatalytic regions enhanced suppression of the yeast mutations, suggesting that these regions might have negative regulatory functions.

We have identified novel tobacco KLPs (designated NACK1 and NACK2) that are involved in the activation of NPK1 and shown that NACK1 regulates the activity and the localization of NPK1 by association through the noncatalytic region of the kinase. Genetic analysis revealed that disruption of NACK1 functions resulted in defects in cytokinesis. Thus, the NACK1/NPK1 complex plays an essential role in the intracellular events that lead to cytokinesis.

Results

Isolation of cDNAs for Activators of NPK1 MAPKKK

To isolate cDNAs for proteins that increased the activity of NPK1, we used a yeast system that exploits a modi-

[3]Correspondence: yas@biol1.bio.nagoya-u.ac.jp
[4]Present address: Department of Biology, University of North Carolina, Chapel Hill, North Carolina 27599.
[5]Present address: College of Bioscience and Biotechnology, Chubu University, 1200 Matsumoto-cho, Kasugai, Aichi 487-8501, Japan.
[6]On leave from Central Research Institute, Ishihara Sangyo Kaisha, Ltd., 2-3-1 Nishi-shibukawa, Kusatsu, Shiga 525-0025, Japan.

fied version of the mating pheromone-responsive MAPK cascade, which consists of STE11 MAPKKK, STE7 MAPKK, and FUS3 MAPK (Irie et al., 1994). Yeast strain SY1984 has a disrupted *STE11* gene and harbors a *HIS3* reporter gene fused to the *FUS1* promoter, which allows examination of the activation of FUS3 MAPK by monitoring the growth of yeast cells on medium prepared without exogenous histidine (Stevenson et al., 1992). We introduced into the SY1984 genome a construct for the constitutive expression of Dsor1^{Su1}, a gain-of-function variant of the Dsor1 MAPKK of *Drosophila* (Tsuda et al., 1993), to enhance the sensitivity of the system to MAPKKK activity. In the resultant strain 11Su1, expression of a truncated, active form of NPK1 that lacked the carboxy-terminal regulatory region allowed cells to grow without exogenous histidine; expression of full-length NPK1 did not (data not shown).

We isolated RNA from actively dividing tobacco BY-2 cells and prepared a plasmid library of cDNAs, all of which would be constitutively expressed in yeast cells. The cDNA library was introduced into 11Su1 cells in which a fusion gene that encoded full-length NPK1 with a galactose-inducible promoter had been integrated. We identified three transformants (#041, #051, and #081) whose growth on histidine-free medium was galactose dependent (Figure 1A; data for #081 not shown), suggesting that the modified yeast MAPK cascade was activated through NPK1 in the presence of the protein encoded by #041, #051, or #081 cDNA.

The 3.2 kb cDNA from clone #051 encoded a predicted protein of 959 amino acid residues (~108 kDa), whose amino-terminal region was homologous to the motor domains that are conserved in members of the KLP family and included amino acid residues that are strongly conserved in various KLPs (Figure 1B). We designated this putative protein *N*PK1-*ac*tivating *k*inesin-like protein *1* (NACK1).

The cDNA from clone #041 (1.3 kb) included a nucleotide sequence that was identical to that of the cDNA from clone #081 (1.0 kb). An open reading frame in cDNA #041 encoded an amino acid sequence similar to that of the carboxy-terminal region of NACK1. We amplified a 2.2 kb fragment of DNA derived from the 5′ end of cDNA #041 by PCR. These cDNAs encoded a predicted protein of 955 amino acids that also had a putative motor domain, and it was designated NACK2 (Figure 1B).

Analysis by the COILS program (Lupas et al., 1991) predicted the presence of several potential coiled coils, typical of the stalk domains in KLPs, in the middle regions of NACK1 and NACK2 (Figure 1C). We shall refer to regions that include coiled coils and carboxy-terminal noncoiled-coil regions as stalk and tail domains, respectively. At the amino acid level, identity between NACK1 and NACK2 was 59% overall, 68% for the amino-terminal putative motor domains, and 55% for the stalk/tail domains.

Two putative *Arabidopsis* KLPs (GenBank accession numbers AAF25984 and CAB89042) exhibited the highest sequence similarities (77% and 65% identical) to NACK1 and NACK2, respectively. We designated them AtNACK1 (its gene maps to chromosome 1) and AtNACK2 (chromosome 3), respectively. Phylogenetic analysis of motor domain sequences indicated that NACK1, NACK2, AtNACK1, and AtNACK2 constitute a subfamily that is closely related to human CENP-E (Yen et al., 1992; Figure 1D). The motor domains of members of the NACK1 subfamily are 41%–44% identical to that of CENP-E. Several other putative KLPs from *Arabidopsis* (e.g., BAA88112) also have motor domains with 45%–51% identity to that of CENP-E. The stalk and tail domains of members of the NACK1 subfamily did not resemble domains of any KLPs in the database.

NACK1 Activates NPK1 Via Direct Interaction

Some MAPKKKs are activated via direct interactions with their activator proteins (Shibuya et al., 1996; Posas and Saito, 1998; Takekawa and Saito, 1998). Therefore, we examined whether a similar mechanism might apply to NPK1 and NACK1.

We performed coimmunoprecipitation analysis using protein extracts from yeast cells that expressed cDNAs for NACK1 and NPK1 separately and together. NPK1 was immunoprecipitated with NPK1-specific antibodies, and immunoprecipitates were analyzed by Western blotting with NACK1-specific antibodies (see below). As shown in Figure 2A, immunoprecipitates contained NACK1 only after NACK1 and NPK1 had been coexpressed, indicating that NACK1 interacted physically with NPK1.

Using a yeast two-hybrid system, we identified the regions required for interactions between NACK1 and NPK1 (data not shown). In NACK1, a 72 amino acid stretch (residues 685–756), corresponding to the fifth putative coiled-coil region and strongly conserved in NACK1 and NACK2, was sufficient for interaction with NPK1 (see Figures 1B and 1C). Conversely, NACK1 binding activity of NPK1 resided in 64 amino acids at the carboxyl terminus (residues 627–690), which also formed a coiled coil (Nishihama et al., 1997, 2001). Using recombinant proteins synthesized in and purified from *Escherichia coli*, we also observed direct interaction in vitro between the stalk/tail region of NACK1 and the regulatory domain of NPK1 by coimmunoprecipitation (data not shown).

An immunocomplex kinase assay of NPK1 with yeast cells expressing NACK1 and/or NPK1 (Figure 2B) revealed strong phosphorylation of myelin basic protein (MBP), as substrate, only when both NACK1 and NPK1 had been produced in yeast cells (lane 3). Very limited phosphorylation was observed in the absence of NACK1 (lane 1). When kinase-negative NPK1 (lanes 2 and 4) or no NPK1 (lane 5) was expressed, similar limited phosphorylation occurred despite the presence of NACK1. Thus, strong phosphorylation of MBP depended on the presence of both NPK1 and NACK1, suggesting that NACK1 might increase the activity of NPK1 via direct interactions between the two proteins. We cannot, however, exclude the possibility that the activation observed in yeast was due to combinatorial effects of some unidentified yeast protein(s).

We observed two additional bands (PB1 and PB2) of phosphorylated proteins when both NACK1 and NPK1 were produced in yeast cells (Figure 2B, top). We concluded that PB1 and PB2 represented phosphorylated forms of NACK1 and NPK1, respectively. When amino-terminally truncated NACK1 (which retained the ability to increase the activity of NPK1) was expressed, we

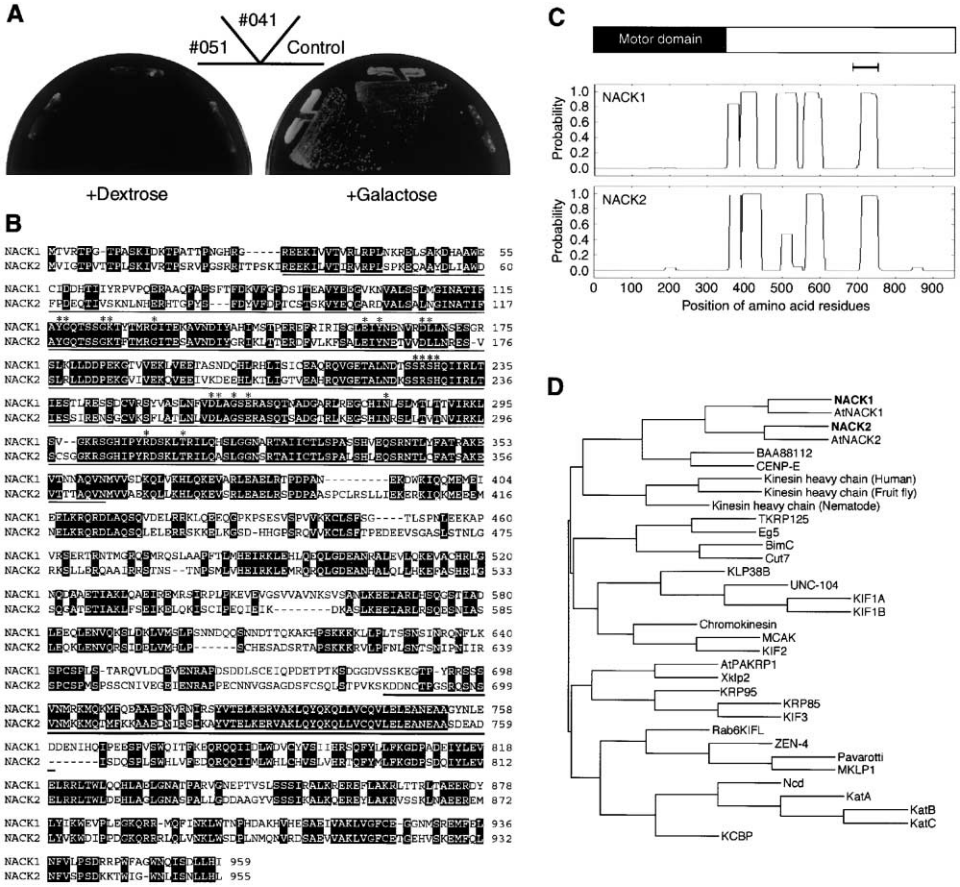

Figure 1. Cloning and Characterization of cDNAs that Encode Activators of NPK1 MAPKKK

(A) Selection of cDNAs for proteins that act as activators of NPK1 in yeast cells. Three yeast clones (#041, #051, and #081) were selected, and plasmids were isolated from them. Yeast cells (11Su1N) were retransformed with the plasmids from clones #041 and #051, as well as with the empty vector (control). Transformants were streaked on histidine-free medium that contained dextrose or galactose and grown at 30°C for 3 days.

(B) Comparison of the deduced amino acid sequences of NACK1 and NACK2. Identical residues are shown in black boxes. Motor domains are underlined by thin lines. Asterisks mark residues conserved in most KLPs and also in NACK1 and NACK2. The NACK1 region responsible for binding to NPK1 is underlined by thick lines.

(C) Prediction of coiled-coil structures. The COILS program (http://www.ch.embnet.org/software/COILS_form.html) was used to calculate probabilities of formation of coiled coils in NACK1 and NACK2 with a window of 28 residues. The box above the graphs shows a schematic representation of the structures of NACK1 and NACK2. A bar shows the region of NACK1 required for binding to NPK1.

(D) Phylogenetic analysis. Amino acid sequences of various KLP motor domains were aligned with the ClustalX program, and the resulting alignment was used to generate a phylogenetic tree with the PHYLIP program package v3.573c (http://evolution.genetics.washington.edu/phylip.html). One thousand replicates of the data set were analyzed.

detected PB2 but not PB1. Instead, we detected a new phosphorylated protein with the greater mobility expected of the truncated NACK1 (data not shown). Moreover, the mobility of a significant fraction of wild-type NPK1 in extracts was reduced when NACK1 had been coexpressed in cells (Figure 2B, bottom, lane 3), while no such mobility shift was observed when kinase-negative NPK1 was expressed, suggesting the catalytic activity-dependent phosphorylation of NPK1. Thus, we propose that NPK1, bound to NACK1, phosphorylates MBP, NACK1, and itself.

NACK1 Is a Mitotic KLP that Associates with NPK1 When Its Activity Is High

We examined the accumulation of *NACK1* and *NACK2* transcripts during the cell cycle. We synchronized the growth of BY-2 cells at the G1/S boundary using aphidicolin. Northern blotting analysis revealed that high levels of transcripts of both *NACK1* and *NACK2* accumulated in cells that had been cultured for 6 to 10 hr after the removal of aphidicolin, with almost the same time course as the change in mitotic indices (MIs; Figure 3A).

We performed Western blotting to examine the accumulation of NACK1 proteins. Affinity-purified antibodies against amino acid residues 385–402 of NACK1 (a synthetic oligopeptide) recognized proteins only in extracts from M phase cells with a mobility that corresponded approximately to that predicted for NACK1 (Figure 3B). After removal of aphidicolin, NACK1 became detectable at 8 hr, reached its highest level at 10 hr, and became undetectable at 14 hr. In the same extracts, we detected NPK1 at a constant level from 0 to 6 hr; the level was

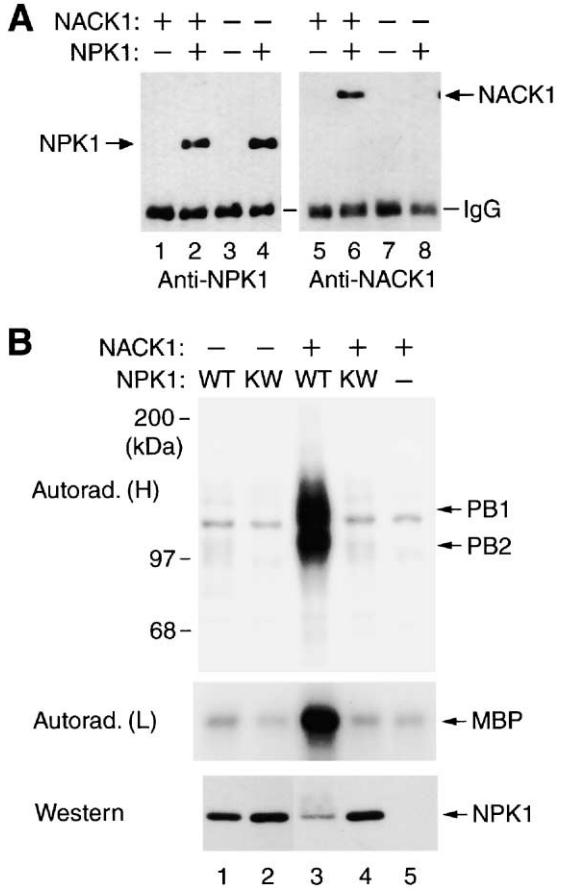

Figure 2. Interaction between NACK1 and NPK1 and Activation of NPK1 by NACK1

(A) Coimmunoprecipitation of NACK1 with NPK1 from extracts of yeast cells. Yeast 11Su1N cells with a galactose-inducible NPK1 construct were transformed with either NACK1-expressing vector (lanes 1 and 2) or the control vector (lanes 3 and 4). Cells were cultured in the presence of dextrose (lanes 1 and 3) or galactose (lanes 2 and 4). Proteins were extracted from cells, and NPK1 was immunoprecipitated with NPK1-specific antibodies. Aliquots of immunoprecipitates were analyzed by Western blotting with NPK1-specific or NACK1-specific antibodies.

(B) Kinase activity in immunocomplexes. Proteins were extracted from yeast SY1984 cells that had been transformed with two plasmids: one was either a NACK1-expressing vector (lanes 3–5) or the control vector (lanes 1 and 2); the other was a wild-type NPK1-expressing vector (lanes 1 and 3), a kinase-negative NPK1-expressing vector (KW; lanes 2 and 4), or the control vector (lane 5). Immunocomplex kinase assays were performed with NPK1-specific antibodies and MBP as substrate. Aliquots of reaction mixtures were subjected to SDS-PAGE (8% [H] and 12% [L] polyacrylamide), and phosphorylated proteins were detected by autoradiography (autorad.). Two major bands of phosphorylated protein are indicated (PB1 and PB2). Yeast protein extracts were also analyzed by Western blotting with NPK1-specific antibodies.

highest at 8 hr, and NPK1 became undetectable at 14 hr, as described previously (Nishihama et al., 2001).

We examined the details of NACK1 accumulation during M phase. BY-2 cells were cultured in synchrony from prometaphase by two-step synchronization with aphidicolin and propyzamide (Kakimoto and Shibaoka, 1988). In the synchronized culture for which results are shown in Figure 3C, more than 50% of cells were in mitosis during the first hour after removal of propyzamide. Then, MIs fell rapidly to the basal value within 3 hr. In these cells, NACK1 was detectable at 0 hr; its level increased during the first hr and then fell rapidly during the next 2 hr (Figure 3C). We showed previously that NPK1 activity is high 1 to 2 hr after the start of synchronization (late M phase; Nishihama et al., 2001). Thus, changes in NPK1 activity were closely correlated with levels of NACK1.

We examined whether NACK1 was associated with NPK1 at the late M phase. We prepared an extract of BY-2 cells that had been harvested 1.5 hr after two-step synchronization. Proteins were immunoprecipitated with NACK1-specific antibodies that had or had not been incubated with the antigenic oligopeptide. Western blotting revealed not only the recovery of NACK1, but also of NPK1 in the precipitate only if antibodies had not been incubated with the oligopeptide (Figure 3D). These data revealed the physical interaction between NACK1 and NPK1 at late M phase in tobacco cells at the time when NPK1 is activated.

NACK1 Is Probably a Plus End-Directed KLP

A protein fraction (E1), purified biochemically from phragmoplasts by following the activity of MT-associated motor proteins, was shown by Asada and Shibaoka (1994) to have plus end-directed motor activity and to consist of polypeptides of 125 kDa and 120 kDa. The 125 kDa protein was the KLP encoded by the *TKRP125* gene (Asada et al., 1997). When we analyzed an E1 fraction by Western blotting with NACK1-specific antibodies, we detected a band at the same position as that of a 120 kDa polypeptide (Figure 3E, lane 2). We repeated Western blotting of the same membrane with TKRP125-specific antibodies without removing the NACK1-specific antibodies and detected a doublet band that corresponded to polypeptides of 125 kDa and 120 kDa (Figure 3E, lane 3). These observations suggested that NACK1 KLP might be a phragmoplast-associated motor protein with plus end-directed motor activity.

NACK1 Is Colocalized with NPK1 at the Phragmoplast Equator

We examined the subcellular localization of NACK1 during M phase by immunofluorescence (Figure 4A). In prophase cells, no NACK1 was clearly detectable. From prometaphase to early anaphase, NACK1 was dispersed in the cytoplasm, yielding patchy signals. At late anaphase, NACK1 accumulated as a band in the spindle midzone. From early to late telophase, NACK1 was consistently localized in the equatorial zone of the phragmoplast; it was colocalized with phragmoplast MTs, but was not found in the inner region of the phragmoplast where the cell plate matures (see late telophase). Incubation of antibodies with the antigenic oligopeptide prior to use abolished the patchy cytoplasmic signals and the signals from the phragmoplast equator (data not shown), confirming that signals of interest were due to NACK1 that was recognized by the antibodies.

We demonstrated previously that green fluorescent protein-fused NPK1 protein (GFP-NPK1) is localized at the equatorial zone of the phragmoplast (Nishihama et al., 2001). When BY-2 cells that expressed GFP-NPK1

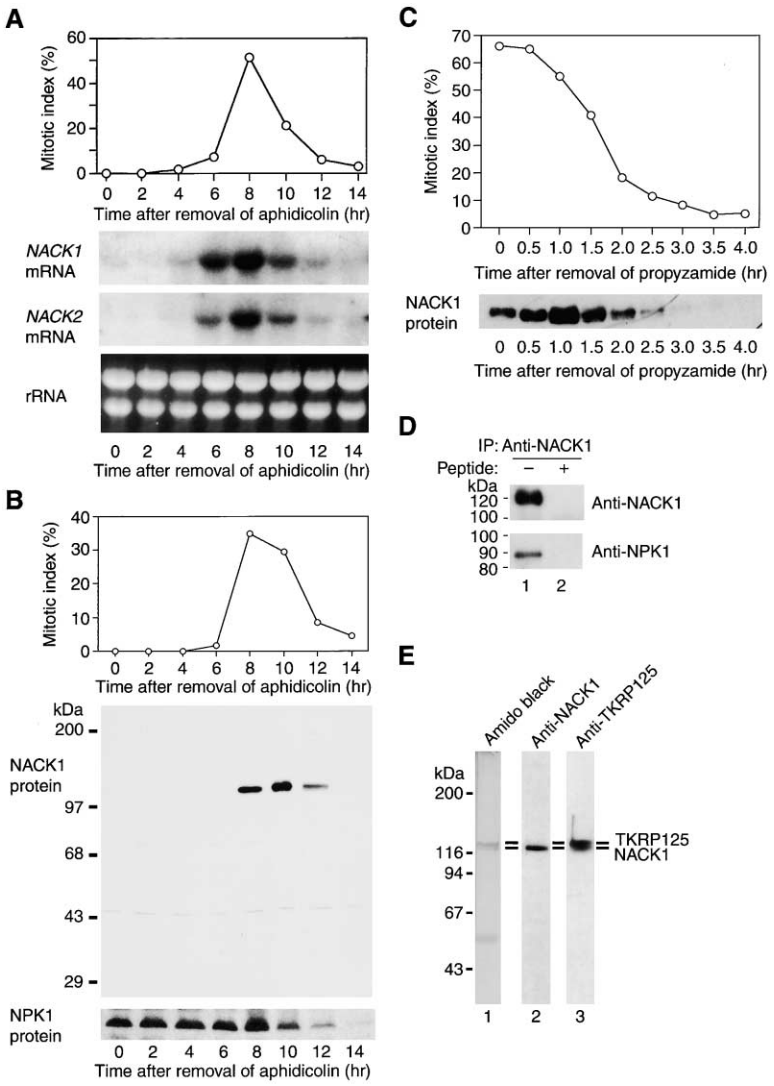

Figure 3. Expression and Immunochemical Analysis of NACK1 in BY-2 Cells

(A) Patterns of accumulation of *NACK1* and *NACK2* transcripts during the cell cycle. The cell cycle was arrested at the G1/S boundary with aphidicolin. At the indicated times (hr) after removal of aphidicolin, cells were harvested and total RNA was extracted. Northern blot analysis was performed with ^{32}P-labeled probes specific to the *NACK1* or *NACK2* gene. MIs are shown in the top panel. Staining of ribosomal RNAs with ethidium bromide is shown in the bottom panel.

(B) Patterns of accumulation of NACK1 during the cell cycle. Proteins were extracted from cells prepared as described in the legend to panel (A). Western blotting was performed with affinity-purified NACK1-specific and NPK1-specific antibodies. MIs are shown in the top panel.

(C) Patterns of accumulation of NACK1 proteins from the M to G1 phase. The cell cycle was arrested at prometaphase with propyzamide after release from the aphidicolin block. At the indicated times (hr) after removal of propyzamide, cells were harvested and proteins were extracted. Western blotting was performed with NACK1-specific antibodies. MIs are shown in the top panel.

(D) Physical interaction of NACK1 with NPK1 at late M phase. Proteins were extracted from BY-2 cells harvested 1.5 hr after release from the propyzamide block. Immunoprecipitation was performed with NACK1-specific antibodies with (lane 2) or without (lane 1) preincubation with the antigenic oligopeptide. Precipitates were analyzed by Western blotting with NACK1-specific and NPK1-specific antibodies.

(E) Putative identification of NACK1 as a plus end-directed motor protein associated with phragmoplasts. A fraction (E1 fraction), containing polypeptides of 125 kDa and 120 kDa with plus end-directed MT motor activity, was isolated from phragmoplasts (Asada and Shibaoka, 1994). Proteins in this fraction were separated by SDS-PAGE and transferred to a nitrocellulose membrane. The membrane was probed with NACK1-specific antibodies (lane 2) and then with TKRP125-specific antibodies (Asada et al., 1997; lane 3). Signals were detected on X-ray film with a chemiluminescence detection kit. Amido black staining of transferred proteins is shown in lane 1. Note the doublet was detected after probing with the two antibodies.

at telophase were double-stained with NACK1-specific antibodies and 4′,6-diamidino-2-phenylindole (DAPI), fluorescent signals derived from GFP and NACK1 were detected as sharp bands at the same position that corresponded to the equatorial zone of the phragmoplast (Figure 4B, left), demonstrating colocalization of the two proteins. Upon expression of a DNA construct that encoded a GFP-fused variant of NPK1 (GFP-NPK1:1–627), which lacked the carboxy-terminal region (residue 628 to the carboxyl terminus) that contains the NACK1 binding site (see above), GFP-NPK1:1–627 was not localized as a sharp band but appeared to be dispersed throughout the cytoplasm, as was GFP alone, while NACK1 was localized as a sharp band in the equatorial zone (Figure 4B, middle and right). These results suggested that NPK1 is recruited to the phragmoplast equator through the carboxy-terminal region, probably via association with NACK1.

Effects of Overexpression of Dominant-Negative *NACK1* Mutant cDNA on Cytokinesis

We postulated that overexpression of truncated NACK1 that lacked the motor domain (NACK1:ST) might disrupt cytokinesis by dominant-negative disturbance of the localization of NPK1. Therefore, we transformed BY-2 cells with a DNA construct for hemagglutinin-tagged NACK1:ST (HA-NACK1:ST), driven by a dexamethasone (DEX)-inducible transcription system (Aoyama and Chua, 1997). We confirmed that overexpressed HA-NACK1:ST was coimmunoprecipitated with endogenous NPK1 (data not shown).

Double staining with Calcofluor and propidium iodide (PI) revealed that approximately 10% of cells became multinucleate upon DEX treatment (Figure 5A, +DEX), with aberrant cell plates of irregular size that resembled those generated upon overexpression of kinase-negative NPK1 (Nishihama et al., 2001). This abnormality was

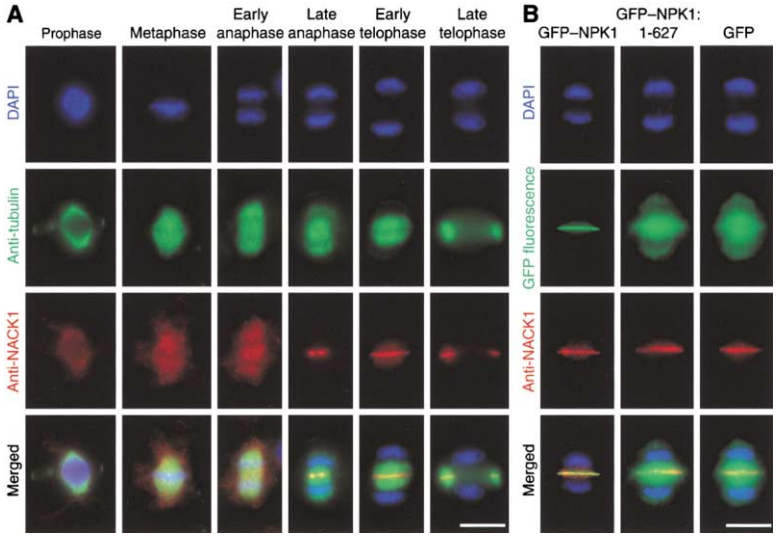

Figure 4. Subcellular Localization of NACK1 and Its Colocalization with NPK1 in BY-2 Cells

(A) Localization of NACK1. BY-2 cells at various phases of the cell cycle were triple stained with NACK1-specific antibodies (red), α-tubulin-specific antibodies (green), and DAPI (blue). Merged images are shown at the bottom.

(B) Colocalization of NACK1 with NPK1 at telophase. BY-2 cells harboring constructs for DEX-inducible GFP-NPK1, GFP-NPK1:1–627, or GFP were treated with aphidicolin. DEX (0.1 μM) was added 12 hr after the start of aphidicolin treatment, and cells were cultured for another 12 hr. After removal of aphidicolin, cells were cultured in fresh medium plus 0.1 μM DEX for 10 hr and double stained with NACK1-specific antibodies (red) and DAPI (blue). Fluorescence of GFP (green) was monitored simultaneously. Merged images are shown at the bottom. Bars are 20 μm.

not observed when transformed cells were not exposed to DEX (Figure 5A, –DEX) or when BY-2 cells were transformed with the control empty vector (Nishihama et al., 2001).

We followed progression of cell plate formation in living cells that had the HA-NACK1:ST construct (Figure 5B). In DEX-untreated cells (–DEX), the cell plate visualized just after chromosome separation (3 min) started lateral expansion immediately, reaching parental cell walls at 23 min. By contrast, a significant proportion of DEX-treated cells exhibited different profiles. In such cells (+DEX), although initial formation of a cell plate (2 min) and its slight enlargement (7 min) occurred, no further expansion was observed for 52 min. Thus, overexpression of HA-NACK1:ST blocked expansion of the cell plate, suggesting that NACK1, together with NPK1

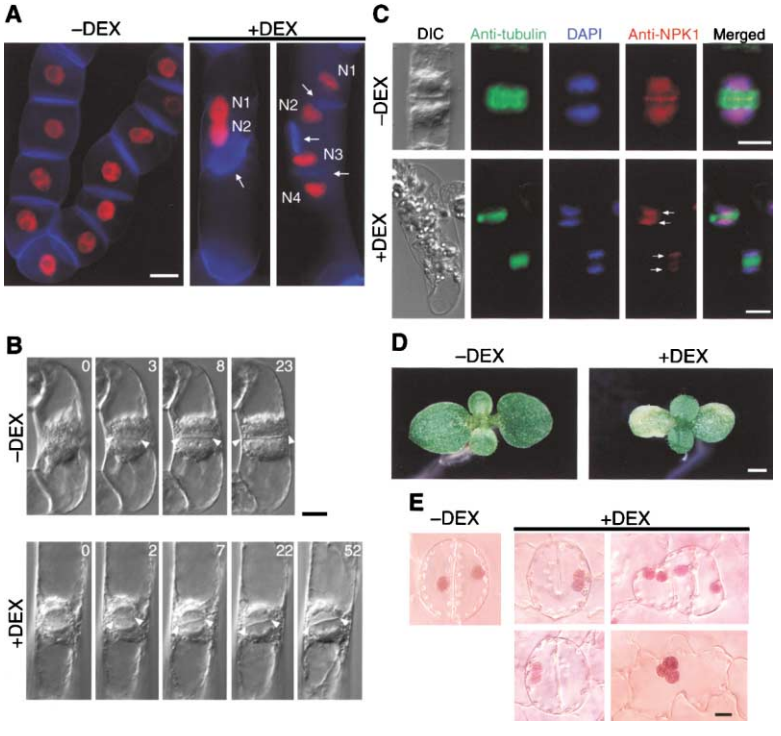

Figure 5. Cytokinetic Defects and NPK1 Mislocalization upon Overexpression of Truncated NACK1

(A) Generation of incomplete cell plates upon overexpression of motor domain-truncated NACK1. BY-2 cells, transformed with a DEX-inducible HA-NACK1:ST construct, were cultured with (+) or without (–) 0.1 μM DEX for 3 days. Cells were fixed and double stained with Calcofluor (blue) and PI (red). Arrows indicate incomplete cell plates. N1 through N4 indicate nuclei found in individual multinucleate cells. Bar is 50 μm.

(B) Time-lapse micrographs of cell-plate formation in living cells. BY-2 cells with DEX-inducible HA-NACK1:ST were cultured with (+) or without (–) 0.1 μM DEX for 2 days. Nomarski images were recorded at indicated times (min) after the start of observation of anaphase cells.

(C) Inhibition of concentration of NPK1 at the phragmoplast upon overexpression of HA-NACK1:ST. Cells, prepared as described in the legend to (A), were triple stained with α-tubulin-specific antibodies (green), DAPI (blue), and NPK1-specific antibodies (red). Merged images are shown on the right. Nomarski images (DIC) are shown on the left. Note the multinucleate cell in the panel labeled +DEX. Arrows indicate multiple nuclei in which NPK1 was concentrated. Bars for (B) and (C) are 20 μm.

(D and E) Generation of multinucleate cells in the epidermis of cotyledons upon expression of HA-NACK1:ST. Seeds of a plant transformed with the DEX-inducible HA-NACK1:ST construct were allowed to germinate on solid medium supplemented with 1 μM DEX (+DEX) or without DEX (–DEX).

(D) Surface views of cotyledons of 10-day-old seedlings. Bar is 1 mm.

(E) Normarski images of guard cells and a pavement cell (bottom right) in orcein-stained cotyledons. Bar is 10 μm.

(Nishihama et al., 2001), is directly involved in expansion of cell plates.

We triple stained cells that expressed HA-NACK1:ST with NPK1-specific antibodies, tubulin-specific antibodies, and DAPI. In multinucleate cells, phragmoplasts formed at telophase and, in a significant proportion of cells, NPK1 was not concentrated at the phragmoplast equator (Figure 5C, +DEX). Cells with such NPK1-negative phragmoplasts were never found in cultures of DEX-untreated cells at telophase (Figure 5C, –DEX). We noted, however, that NPK1 concentrated in pairs of daughter nuclei even when cells were treated with DEX (arrows in Figure 5C). These results indicated that NACK1 functions by recruiting NPK1 to the phragmoplast equator, as proposed above. Inappropriate localization of NPK1 might have been one of the causes of imperfect formation of a cell plate in cells that expressed HA-NACK1:ST.

To examine whether overexpression of HA-NACK1:ST can disturb NACK1 functions in plants, we prepared transgenic tobacco plants that harbored DEX-inducible HA-NACK1:ST. After germination on DEX-containing medium, cotyledons of such plants developed with rough surfaces and were sometimes etiolated (Figure 5D, +DEX). Epidermal cells in cotyledons were most severely affected (Figure 5E, +DEX): 50% of pavement cells were multinucleate; 25% of guard cells were binucleate; some cells were anucleate; and, in some cells, cytokinesis was incomplete or absent. Such phenotypes can be explained by the arrest or delay of cytokinesis during the development of pavement and guard cells. No abnormalities were seen in cotyledons of transgenic plants in the absence of DEX (Figures 5D and 5E, –DEX). Similar defects were seen in cotyledons of transgenic tobacco plants that expressed the kinase-negative mutant of NPK1 (Nishihama et al., 2001).

Loss-of-Function Phenotypes Caused by Silencing of *NACK1* and *NACK2*

To analyze phenotypes caused by loss of function of *NACK1*, we exploited a virus-induced gene-silencing (VIGS) system using potato virus X (PVX; Angell and Baulcombe, 1999). Since possible functional redundancy between *NACK1* and *NACK2* might attenuate the severity of defects, we attempted to repress expression of both genes simultaneously. Fragments of *NACK1* and *NACK2* cDNAs were introduced downstream of the T7 promoter in a PVX vector (Baulcombe et al., 1995), in tandem, in the sense orientation. GFP cDNA was introduced into the same site in the vector as a control. PVX-NACK1/NACK2 or PVX-GFP transcripts, synthesized in vitro, were inoculated onto leaves of *Nicotiana benthamiana* plants. Fourteen days postinoculation (DPI), mild mosaic symptoms appeared on the upper leaves in both series of inoculated plants. PVX-NACK1/NACK2 RNA was detected by reverse transcription-PCR (RT-PCR) in such leaves on PVX-NACK1/NACK2 RNA-inoculated plants, and fluorescence due to GFP was detected in leaves of the control plants (data not shown), indicating successful infection.

By 21 DPI with PVX-NACK1/NACK2 RNA, retardation of growth was apparent in five out of nine infected plants, which finally stopped growing (Figure 6A; plants at 30 DPI). All such arrested plants generated small, humped leaves at a position above inoculated leaves, and these malformed leaves remained small (Figure 6A, part 1). Their one or two abortive flower buds had morphologically normal sepals but prematurely terminated petals, stamens, and gynoecia, which eventually underwent necrosis (Figure 6A, part 2; aborted stamens not visible). By contrast, all of the nine PVX-GFP RNA-infected plants grew normally and generated five to six flower buds by 30 DPI (Figure 6A). Therefore, the growth defect seemed to be induced by infection with PVX-NACK1/NACK2 RNA and not by disease due to PVX.

We investigated cytokinesis in plants with a growth defect by examining guard cells in leaves. As shown in Figure 6B, 20% to 50% of guard mother cells did not divide to generate guard cells and had two nuclei (Figure 6B, parts 2–4). Some guard cells had incomplete cell walls (Figure 6B, parts 2 and 3). PVX-GFP RNA-infected plants developed guard cells normally (Figure 6B, part 1). Thus, cytokinesis during development of guard cells was inhibited in malformed leaves after infection with PVX-NACK1/NACK2 RNA. Using RNA isolated from tissues in the shoot apex (including small leaves) as template for RT-PCR, we examined levels of *NACK1* and *NACK2* transcripts derived from the respective endogenous genes. Levels of *NACK1* and *NACK2* transcripts of the endogenous genes in PVX-NACK1/NACK2 RNA-infected plants with the phenotypes fell to the limit of detection, while such transcripts in PVX-NACK1/NACK2 RNA-infected plants without the phenotypes, PVX-GFP RNA-infected plants or uninfected plants were clearly detected (Figure 6C).

Our results suggested that the infection with PVX-NACK1/NACK2 RNA silenced expression of *NACK1* and *NACK2* genes, with resultant cytokinetic defects during leaf production and, probably, in floral organs. Phenotypes after *NACK1*/*NACK2* VIGS were compatible with those observed after overexpression of dominant-negative *NACK1* cDNA, suggesting that abnormal phenotypes were not caused by artifacts due to overexpression. However, it remains to be determined whether the growth defect of lateral organs and plant bodies would be due to direct effects of the cytokinetic defect caused by VIGS.

Disruption of *AtNACK1* Causes Cytokinetic Defects in *Arabidopsis* Embryos

Using PCR-based screening, we identified two mutant alleles of the *AtNACK1* gene (see Figure 1D), *atnack1-1* and *atnack1-2*, with T-DNA insertions in the putative 5th and 12th exons that encode parts of the motor domain and the stalk region, respectively (Figure 7A).

Homozygous *atnack1-1* mutants exhibited growth defects, and plants were dwarfed with small, humped cotyledons and leaves (Figure 7B). Development of *atnack1-1* plants ceased at the vegetative stage, and they died without any traces of production of reproductive organs (data not shown). The *atnack1-2* plants had essentially identical defects (data not shown). Therefore, both alleles were maintained in heterozygous plants, which were morphologically indistinguishable from wild-type plants.

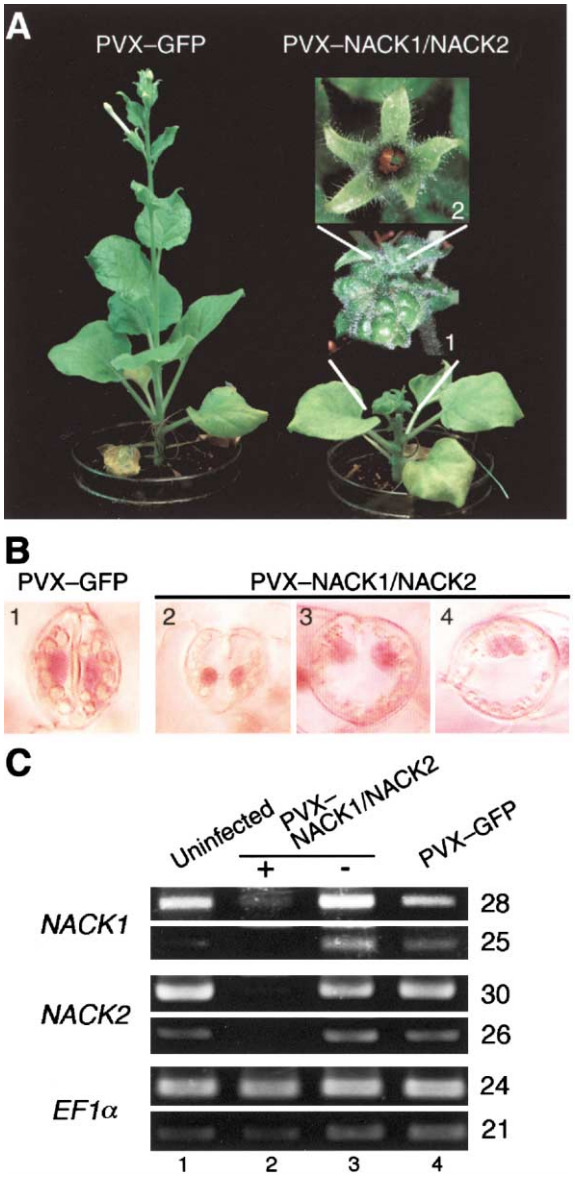

Figure 6. Phenotypes Generated by Suppression of *NACK1* and *NACK2*

(A) Leaves of 1-month-old plants of *N. benthamiana* were inoculated with PVX-NACK1/NACK2 or PVX-GFP RNA. Gross morphology of typical plants, 30 DPI, is shown. The insets show magnified views of the shoot apex (part 1) and an aborted flower (part 2) of a PVX-NACK1/NACK2 RNA-inoculated plant. Necrotic petals (brown) and small green carpels are visible.

(B) Nomarski images of orcein-stained guard cells on the second highest leaves of a PVX-GFP-infected plant (part 1) and a PVX-NACK1/NACK2 RNA-infected plant (parts 2–4), 30 DPI. These are the same plants as shown in (A).

(C) RT-PCR analysis. RNA was prepared from shoot apices containing small leaves, of an uninfected plant (lane 1), of a plant with a growth defect (+) 35 DPI with PVX-NACK1/NACK2 RNA (lane 2), of a plant with a normal phenotype (–) 35 DPI with PVX-NACK1/NACK2 RNA (lane 3), or of a PVX-GFP RNA-inoculated plant (lane 4). RT-PCR was performed for *NACK1* (top), and *NACK2* (middle) with primers designed to amplify cDNAs derived only from endogenous genes and for *EF1*α as control (bottom). Numbers of cycles of PCR are indicated on the right.

When heterozygous *atnack1-1* and *atnack1-2* plants were self-pollinated, 18.8% (n = 213) and 20.7% (n = 285) of their progeny, respectively, exhibited a mutant phenotype 10 days after germination on solid medium, indicating the recessive nature of the mutation. Genetic linkage analysis of *atnack1-1* (no recombinant/140 meioses) indicated that the mutation was closely linked to the T-DNA insertion in the *AtNACK1* gene. In addition, a normal phenotype was restored by a transgene that contained the *AtNACK1* genomic region (data not shown). Thus, the T-DNA inserted in the *AtNACK1* gene was responsible for the observed phenotype.

The morphological defects in cotyledons of *atnack1* mutants were apparent immediately after germination, so we examined the morphology of embryonic cells in seeds collected from plants heterozygous for the *atnack1-1* or *atnack1-2* mutation. Some seeds (20.1% [n = 199] for *atnack1-1*; 22.7% [n = 229] for *atnack1-2*) contained malformed embryos composed of cells with single nuclei and some multinucleate cells with incomplete cell walls (Figure 7C), indicating the occasional failure in cytokinesis during embryogenesis. It is possible that successful cytokinetic events were due to redundant functions of the *AtNACK2* gene. Our observations suggested that mutations in the *AtNACK1* gene resulted in a defect in the production of cell walls, which was, at least in part, responsible for the phenotypes of mutant seedlings. Thus, the *AtNACK1* gene is required for proper cytokinesis, and the functions of *NACK1*-related genes are conserved in different plant species.

Discussion

Molecular Mechanism of Activation of NPK1 by NACK1

Our genetic (Figure 1A) and biochemical (Figure 2B) evidence indicates that NACK1 is essential for activation of NPK1 in yeast cells, and considerable evidence indicates that NACK1 binds to NPK1 in vivo and in vitro. Therefore, NACK1 probably activates NPK1 via direct interaction.

NACK1 binds to the carboxy-terminal negative-regulatory domain of NPK1, perhaps via interaction between coiled coils formed by 72 amino acids in the stalk region of NACK1 (Figure 1C) and 64 amino acids at the carboxyl terminus of NPK1 (Nishihama et al., 1997). Association of NPK1 with NACK1 might release NPK1 from an inactive conformation. However, the extent of suppression of mutations in yeast MAPKKK genes by coexpression of wild-type NPK1 and NACK1 was greater than that observed upon expression exclusively of the truncated NPK1 (data not shown), suggesting that the release, alone, of the catalytic domain from auto-inhibition conferred by the regulatory domain is insufficient for full activation of NPK1. Autophosphorylation of NPK1 and phosphorylation of NACK1 by NPK1 might occur when these proteins have already formed a complex (Figure 2). Hence, the activity of NPK1 might be further enhanced by autophosphorylation and the action(s) of phosphorylated NACK1, as proposed for other MAP-KKKs (Posas and Saito, 1998; Kishimoto et al., 2000; Sakurai et al., 2000).

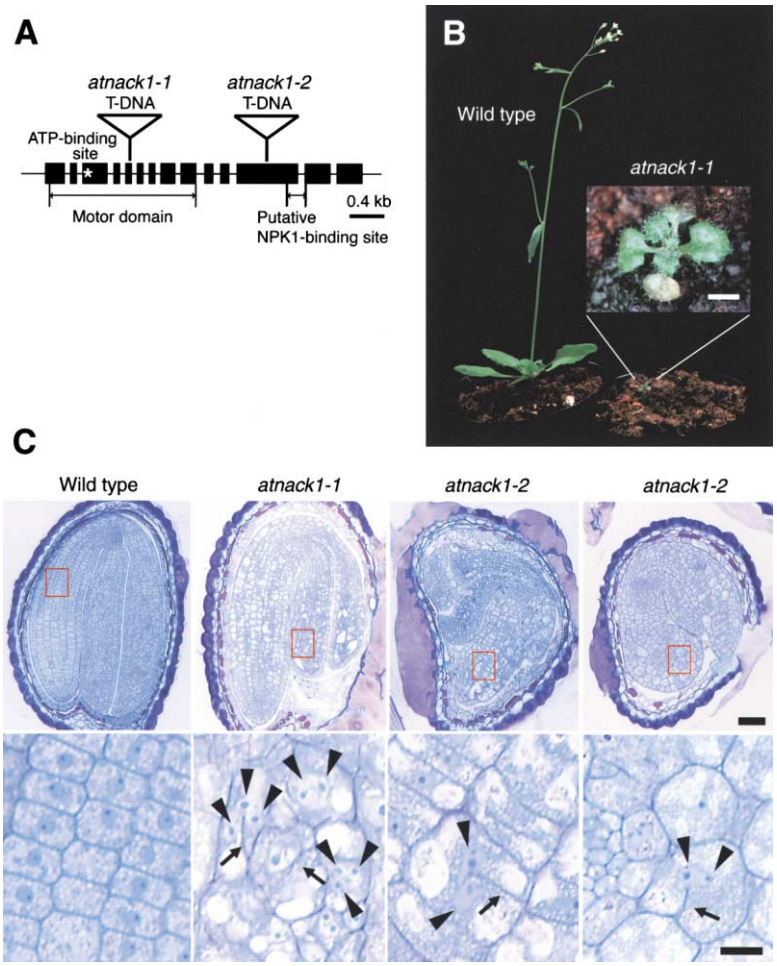

Figure 7. Mutations in the *AtNACK1* Gene Affect Cytokinesis

(A) Schematic diagram of the *AtNACK1* gene. Boxes represent exons. The putative motor domain, ATP binding site (asterisk), and NPK1 binding site are indicated. T-DNA insertion sites in *atnack1-1* and *atnack1-2* are also shown. T-DNA inserts are not drawn to scale.

(B) Gross morphology of wild-type (ecotype Wassilewskija) and *atnack1-1* plants 23 days after germination. Inset: magnified view of the mutant. Bar is 1 mm.

(C) Sections of wild-type and *atnack1* mature seeds stained with toluidine blue. Top: Whole views of single seeds. Bottom: Magnified views of boxed regions in corresponding upper images. Longitudinal sections of hypocotyls (wild-type and *atnack1-2* [left]) and a cotyledon (*atnack1-1*) and a transverse section of a hypocotyl (*atnack1-2* [right]) are shown. Arrows indicate incomplete cell walls. Arrowheads indicate nuclei in multinucleate cells. Bar for (Top) is 50 μm. Bar for (Bottom) is 10 μm.

M Phase-Specific Expression of *NACK1* and *NACK2*

It is concluded that NACK1-mediated activation of NPK1 occurs at the end of M phase since, at this time, the activity of NPK1 (Nishihama et al., 2001) and the level of NACK1 (Figure 3C) are both highest and moreover, these proteins associate (Figure 3D). The M phase-specific accumulation of NACK1 proteins is, at least in part, attributed to that of *NACK1* transcripts (Figure 3A). Transcription of the *NACK1* and *NACK2* genes is regulated by *cis* elements known as M-specific activators (MSAs; Ito et al., 1998). Recently, MSA-dependent transcription has been shown to be controlled by novel c-Myb-like transcription factors (Ito et al., 2001). Detailed mechanisms for the regulation of MSA-dependent transcription by such proteins must be clarified if we are to understand the temporal regulation of the expression of *NACK1* and *NACK2*.

NACK1-Related KLPs Unique to Plants

A few KLPs, such as KIF3X and kinesin-I, are involved in regulation of the transport or localization of components of MAPK cascades (Nagata et al., 1998; Verhey et al., 2001). However, no KLPs have been reported, to our knowledge, to activate associated protein kinases. Animal KLPs in the MKLP1 family concentrate at the spindle midzone and the midbody; they are essential for organization of midzone MTs and subsequent constriction of dividing cells during cytokinesis (Adams et al., 1998; Raich et al., 1998). Some members of this family colocalize with Polo-like kinases or Aurora kinases, which are also required for cytokinesis (Lee et al., 1995; Adams et al., 1998; Severson et al., 2000).

These features of the MKLP1 family are similar to those of NACK1. However, amino acid sequences of motor domains indicate that NACK1 does not belong to the MKLP1 family but is most closely related to CENP-E (Figure 1D), which concentrates at the spindle midzone and the midbody during late M phase (Yen et al., 1991) and associates with a MAPK (Zecevic et al., 1998). It remains unclear whether CENP-E associates with a MAPKKK and/or whether it plays a role in cytokinesis. We were unable to demonstrate the centromeric localization of NACK1. NACK1-related KLPs in plants might participate in a process unique to plant cytokinesis.

The Role of the NACK1/NPK1 Complex in Cell Plate Formation

The key site for cell plate formation is the equatorial zone of the phragmoplast, where two bundles of MTs are arranged with interdigitating plus ends. Lateral expansion of the cell plate is accompanied by MT disas-

sembly at the inside and MT reassembly at the outside of the phragmoplast. When depolymerization of phragmoplast MTs is blocked by taxol, phragmoplasts no longer expand laterally and, coincidentally, incomplete cell plates are formed, indicating that phragmoplast expansion requires disassembly of MTs and allows the cell plate to expand (Yasuhara et al., 1993).

We showed previously that overexpression of kinase-negative NPK1 inhibits expansion of both the phragmoplast and the cell plate, as does taxol, suggesting a role for NPK1 in regulation of the dynamics of phragmoplast MTs (Nishihama and Machida, 2001; Nishihama et al., 2001). We demonstrated here that overexpression of dominant-negative NACK1 inhibits expansion of the cell plate (Figure 5B), a phenomenon that suggests that NACK1 is involved in the same process as NPK1. Thus, NACK1, complexed with NPK1, might regulate depolymerization of MTs during phragmoplast expansion. This hypothesis is supported by the observation that *N. benthamiana* plants in which *NACK1* and *NACK2* expression was repressed by VIGS developed multinucleate guard cells (Figure 6) and that *Arabidopsis atnack1* mutant embryos contained cells with multiple nuclei and cell wall stubs (Figure 7).

Recently, Strompen et al. (2002) have reported that plant cytokinesis requires HINKEL (HIK) KLP of *Arabidopsis*, which is identical to AtNACK1 we identified. Phenotypes of *hik* mutants are consistent with our results, including those of *atnack1-1* and *atnack1-2* (e.g., the generation of multinucleate cells and incomplete cell walls), except that only fully expanded phragmoplasts were found in embryo cells of *hik*. The presence of such phragmoplasts seems to be somewhat different from the results of the arrest of cell plate and phragmoplast expansion by kinetic analyses upon expression of the dominant inhibitory NACK1:ST (Figure 5B) and NPK1KW (Nishihama et al., 2001), respectively. This might be due to different experimental systems; in our experiments with tobacco cells and plants, functions of both *NACK1* and *NACK2* may have been interfered with by the dominant-negative forms and VIGS, while *AtNACK2* may have replaced at least in part functions of *HIK* and *AtNACK1* in *Arabidopsis*.

During telophase, both NACK1 and NPK1 are concentrated at the equator of the phragmoplast. We propose that NPK1 is transported by NACK1 for the following reasons. First, truncated NPK1 proteins lacking the NACK1 binding site were incapable of equatorial localization (Figure 4B). Second, truncated NACK1 proteins that lacked the motor domain prevented localization of NPK1 to the phragmoplast equator (Figure 5C). Movement of NACK1 to the plus ends of phragmoplast MTs appears to involve its motor activity and, indeed, NACK1 was purified from phragmoplasts in a fraction with plus end-directed motor activity (Figure 3E).

The activity and positioning of NPK1 appear to be critical for cytokinesis. Activation of NPK1 by binding to KLPs, such as NACK1 that is localized to the phragmoplast equator could provide a simple and robust mechanism for precise regulation of NPK1. How might NPK1 signaling be involved in cell plate formation? We recently identified a MAPKK (NQK1) and a MAPK (NRK1) as putative factors that act downstream of NPK1 (T.S., R.N., and Y.M., unpublished data). We shall try to determine whether these kinases, and also p43^{Ntf6} (Calderini et al., 1998), are involved in cell plate formation and function downstream of NPK1. However, one target of NPK1 might be a regulator of MT dynamics. Some KLPs have MT-depolymerizing activity (Hunter and Wordeman, 2000). Since NPK1 can phosphorylate NACK1, it is possible that NACK1, phosphorylated by NPK1, might control MT dynamics. Further investigation on functions of NACK1 and NPK1 should help to clarify mechanisms for the inside-out nature of cell plate expansion.

Experimental Procedures

Plant and Yeast Materials

Maintenance and transformation of *Nicotiana* plants (*N. tabacum* SR1 and *N. benthamiana*), BY-2 tobacco cultured cells, and *Arabidopsis thaliana* plants are described elsewhere (Nishihama et al., 2001; Tanaka et al., 2001). *Saccharomyces cerevisiae* SY1984 (*MAT*α *leu2 ura3 trp1 his3*Δ*::ura3 pep4*Δ*::ura3 can1 FUS1::HIS3 ste11*Δ*::ura3*; Stevenson et al., 1992) was used for preparation of 11Su1 cells, in which *CYC1* promoter-fused Dsor1^{Su1} cDNA (Tsuda et al., 1993) was integrated at the *trp1* locus. *GAL1* promoter-fused NPK1 cDNA was integrated at the *leu2* locus of 11Su1 to generate 11Su1N cells.

Isolation of Tobacco cDNAs for Activators of NPK1 Using Yeast Cells

Total RNA from BY-2 cells, 3 days after subculture, was isolated, and poly(A)$^+$ RNA was purified as described elsewhere (Banno et al., 1993). cDNAs were synthesized from the poly(A)$^+$ RNA and cloned into plasmid pKT11 (*URA3* marker; see below). Yeast 11Su1N cells were transformed with the cDNA library and grown on synthetic galactose (SG) medium without tryptophan (Trp), leucine (Leu), uracil (Ura), and histidine (His) at 30°C. Of 3×10^5 transformants, 150 clones formed colonies within 2 weeks. These clones were further selected for failure to grow on synthetic dextrose (SD) medium without Trp, Leu, Ura, and His and for failure to grow on SG medium without Trp, Leu, and His after cells had been cured of plasmids by treatment with 5-fluoroorotic acid.

Construction of Plasmids

A linker fragment, prepared by annealing the oligonucleotides 5′-AATTGGTCGACGAATTCTCTAGAGCGGCCGC-3′ and 5′-TCGAG CGGCCGCTCTAGAGAATTCGTCGACC-3′, was inserted into pKT10 (Tanaka et al., 1989) that had been digested with EcoRI and SalI to yield pKT11. YCpGT (*TRP1* marker) was generated by inserting a SalI-NdeI (filled-in) fragment of pGT5 (Miyajima et al., 1987) into the SalI and filled-in EcoRI sites of YCplac22 (Gietz and Sugino, 1988). YCpGT-NPK1 and YCpGT-NPK1KW were generated by inserting an XbaI-StuI fragment of pNPK1-#6 (Banno et al., 1993) or pNPK1KW (Nishihama et al., 2001), respectively, into YCpGT that had been digested with XbaI and SmaI. For DEX-inducible expression of proteins in BY-2 cells, DNA encoding HA-NACK1:ST or GFP-NPK1:1–627 was cloned into pTA7001 (Aoyama and Chua, 1997) to yield pTA71-HA-NACK1:ST and pTA71-GFP-NPK1:1–627, respectively. To generate PVX constructs using the pP2C2S vector (Baulcombe et al., 1995), we amplified a 380 bp fragment of *NACK1* cDNA and a 358 bp fragment of *NACK2* cDNA, which both include regions encoding the NPK1 binding sites, by PCR, using oligonucleotide primers N1F2194 (5′-GCCGTTCCAGTTCTGTGAAC-3′) and N1R2573 (5′-AGTTCAACTTCCAGATATATTTC-3′) for *NACK1* and N2F2175 (5′-GGCAGTCAAACTCTGTTAAT-3′) and N2R2532 (5′-AGCTCAACTTCCAAGTATATC-3′) for *NACK2*. Both were inserted into pP2C2S such that they were arranged in the sense orientation downstream of the T7 promoter to yield pP2C2S-NACK1/NACK2. GFP cDNA (Chiu et al., 1996) was introduced into pP2C2S to yield pP2C2S-GFP. Details of construction of these plasmids are available on request.

Production and Purification of Antibodies

Antibodies against NACK1 were prepared by MBL (Nagoya, Japan) with a synthetic peptide, CTPDPANEKDWKIQQMEME (residues

385–402 of NACK1), as antigen. Specific antibodies were affinity-purified with the antigenic oligopeptide (Nishihama et al., 2001).

Coimmunoprecipitation and Immunocomplex Kinase Assays

We cultured yeast 11Su1N cells that harbored pKT11-051 or pKT11 in 50 ml of liquid SD or SG medium without Trp, Leu, and Ura until absorbance at 600 nm reached 1.0. Cells were washed twice with chilled water and resuspended in 500 μl of TG250Y buffer (TG250 buffer [Nishihama et al., 2001] prepared with 15 mM, instead of 10 mM, EGTA, and without EDTA and bovine serum albumin [BSA]). Cells were disrupted with glass beads. Cleared lysates containing 400 μg of protein were diluted with 500 μl of T150Y buffer (TG250Y buffer prepared with 150 mM NaCl instead of 250 mM NaCl and without glycerol) and incubated with 1 μg of NPK1-specific antibodies (P557-2; Nishihama et al., 2001) on ice for 90 min, followed by 60 min incubation at 4°C with 20 μl of a 50% slurry of protein A-Sepharose (Amersham Pharmacia Biotech, Piscataway, NJ). The resin was washed four times in T150Y buffer, resuspended in 80 μl of 1× sample buffer for SDS-PAGE, and boiled.

For assays of kinase activity, yeast SY1984 cells harboring YCpGT, YCpGT-NPK1, or YCpGT-NPK1KW plus either pKT11 or pKT11-051 were cultured in 50 ml of SG medium without Trp and Ura. NPK1 was immunoprecipitated from extracts (500 μg of protein), as described above. The resin was washed four times in T150Y buffer and twice in kinase buffer (Nishihama et al., 2001). Precipitates were resuspended in a reaction cocktail (20 μl) that included 1 μg of MBP (Sigma, St. Louis, MO), 50 μM ATP, and 10 μCi of [γ-^{32}P]ATP in kinase buffer and incubated for 30 min at 25°C.

Coimmunoprecipitation analysis with BY-2 cells was performed as follows. Frozen BY-2 cells were ground to a powder in liquid nitrogen. The powder was suspended in an equal volume of PG150 buffer (TG250 buffer [Nishihama et al., 2001] prepared with 20 mM PIPES [pH 6.2] instead of 25 mM Tris-HCl [pH 7.5] and 150 mM NaCl instead of 250 mM NaCl, without BSA). Cleared lysate containing 6 mg of protein was incubated on ice for 2 hr with 2 μg of NACK1-specific antibodies that had or had not been incubated with a 70-fold molar excess of antigenic oligopeptide. Precipitates were prepared as described above with PG150 buffer for washing and resuspension in 30 μl of 1× sample buffer for SDS-PAGE.

Northern Blotting Analysis

Northern blotting was performed with total RNA (10 μg) from synchronized BY-2 cells using ^{32}P-labeled gene-specific probes for *NACK1* and *NACK2* (SacI-BstPI and StyI-BsmI segments of the respective cDNAs) as described elsewhere (Banno et al., 1993).

VIGS Technology

VIGS technology is described in detail on the Internet (http://www.jic.bbsrc.ac.uk/Sainsbury-Lab/david-baulcombe/objectives/gstech.htm). Infectious PVX RNAs were transcribed in vitro with pP2C2S-NACK1/NACK2 or pP2C2S-GFP DNA as template. Leaves of nine *N. benthamiana* plants were inoculated with transcribed RNAs. Inoculated plants were grown with 16 hr of light daily at 23°C in a growth chamber. Levels of transcripts of endogenous *NACK1* and *NACK2* genes were examined by quantitative RT-PCR (Semiarti et al., 2001) using primers NAK1-2091F (5′-TAGAGCTCCAGATTCG GATG-3′) and NAK1-3081R (5′-CCAAAATTGGGAGGCTCCAG-3′) for *NACK1* and NAK2-1810F (5′-TGCACGGCTGAGATCTCAGG-3′) and NAK2-2740R (5′-TCCATCAGGTGGAATGTCCC-3′) for *NACK2*. To detect levels of control *EF1*α transcripts, we used primers EFF (5′-AGACCACCAAGTACTACTGC-3′) and EFR (5′-GTCAAGAGCCT CAAGGAGAG-3′) (Ingram et al., 1999).

Isolation of T-DNA-Tagged *atnack1* Mutants

We screened 133,440 T-DNA-tagged *Arabidopsis* plants generated at the *Arabidopsis* Knockout Facility in the University of Wisconsin (60,480 lines from the ALPHA population; Krysan et al., 1999; 72,960 lines from the BASTA population) for *atnack1* mutations by PCR according to the instructions of www.biotech.wisc.edu/*Arabidopsis*. Primers specific for the T-DNA left-border (5′-CATTTTATAATAACG CTGCGGACATCTAC-3′) and *AtNACK1* (AtNA1-1F, 5′-ACCTTTT TATGGATTAAGTCTGCACAATG-3′ and AtNA1-1R, 5′-CATAATCA GACGAGTCTGGTAAAGCTTAT-3′) were used.

Microscopy

All techniques for microscopic analysis were described previously (Nishihama et al., 2001; Tanaka et al., 2001). Sections of *Arabidopsis* seeds were made from siliques that were collected and fixed 7 days after flowering.

Acknowledgments

The authors thank Kunihiro Matsumoto for the yeast screening system; David Baulcombe for the PVX vector (pP2C2S); Shoji Sonoda and Masamichi Nishiguchi for providing *N. benthamiana* plants and helpful discussions; Hiroki Yasuhara, Takahide Yokoi, Keisuke Matsui, and Toshiya Muranaka for technical assistance and helpful discussions; and Sangho Jeong for critical reading of the manuscript. This work was supported by Grants-in-Aid for Scientific Research on Priority Areas (0678101-3 and 10182101-2) from the Japanese Ministry of Education, Science, Culture, and Sports and by a grant from the Research for the Future Program of the Japan Society for the Promotion of Science (JSPS). R.N. was supported by Research Fellowships from JSPS.

Received: September 17, 2001
Revised: February 28, 2002

References

Adams, R.R., Tavares, A.A., Salzberg, A., Bellen, H.J., and Glover, D.M. (1998). *pavarotti* encodes a kinesin-like protein required to organize the central spindle and contractile ring for cytokinesis. Genes Dev. *12*, 1483–1494.

Angell, S.M., and Baulcombe, D.C. (1999). Technical advance: potato virus X amplicon-mediated silencing of nuclear genes. Plant J. *20*, 357–362.

Aoyama, T., and Chua, N.-H. (1997). A glucocorticoid-mediated transcriptional induction system in transgenic plants. Plant J. *11*, 605–612.

Asada, T., and Shibaoka, H. (1994). Isolation of polypeptides with microtubule-translocating activity from phragmoplasts of tobacco BY-2 cells. J. Cell Sci. *107*, 2249–2257.

Asada, T., Kuriyama, R., and Shibaoka, H. (1997). TKRP125, a kinesin-related protein involved in the centrosome-independent organization of the cytokinetic apparatus in tobacco BY-2 cells. J. Cell Sci. *110*, 179–189.

Assaad, F.F., Huet, Y., Mayer, U., and Jürgens, G. (2001). The cytokinesis gene *KEULE* encodes a Sec1 protein that binds the syntaxin KNOLLE. J. Cell Biol. *152*, 531–543.

Banno, H., Hirano, K., Nakamura, T., Irie, K., Nomoto, S., Matsumoto, K., and Machida, Y. (1993). *NPK1*, a tobacco gene that encodes a protein with a domain homologous to yeast BCK1, STE11, and Byr2 protein kinases. Mol. Cell. Biol. *13*, 4745–4752.

Baulcombe, D.C., Chapman, S., and Santa Cruz, S. (1995). Jellyfish green fluorescent protein as a reporter for virus infections. Plant J. *7*, 1045–1053.

Bögre, L., Calderini, O., Binarova, P., Mattauch, M., Till, S., Kiegerl, S., Jonak, C., Pollaschek, C., Barker, P., Huskisson, N.S., et al. (1999). A MAP kinase is activated late in plant mitosis and becomes localized to the plane of cell division. Plant Cell *11*, 101–113.

Calderini, O., Bögre, L., Vicente, O., Binarova, P., Heberle-Bors, E., and Wilson, C. (1998). A cell cycle regulated MAP kinase with a possible role in cytokinesis in tobacco cells. J. Cell Sci. *111*, 3091–3100.

Chiu, W., Niwa, Y., Zeng, W., Hirano, T., Kobayashi, H., and Sheen, J. (1996). Engineered GFP as a vital reporter in plants. Curr. Biol. *6*, 325–330.

Field, C., Li, R., and Oegema, K. (1999). Cytokinesis in eukaryotes: a mechanistic comparison. Curr. Opin. Cell Biol. *11*, 68–80.

Gietz, R.D., and Sugino, A. (1988). New yeast-*Escherichia coli* shuttle vectors constructed with *in vitro* mutagenized yeast genes lacking six-base pair restriction sites. Gene *74*, 527–534.

Gunning, B.E.S. (1982). The cytokinetic apparatus: its development

and spatial regulation. In The Cytoskeleton in Plant Growth and Development, C.W. Lloyd, ed. (London: Academic Press), pp. 229–292.

Heese, M., Mayer, U., and Jürgens, G. (1998). Cytokinesis in flowering plants: cellular process and developmental integration. Curr. Opin. Plant Biol. *1*, 486–491.

Hunter, A.W., and Wordeman, L. (2000). How motor proteins influence microtubule polymerization dynamics. J. Cell Sci. *113*, 4379–4389.

Ingram, R., Charrier, B., Scollan, C., and Meyer, P. (1999). Transgenic tobacco plants expressing the *Drosophila* Polycomb (Pc) chromodomain show developmental alterations: possible role of Pc chromodomain proteins in chromatin-mediated gene regulation in plants. Plant Cell *11*, 1047–1060.

Irie, K., Gotoh, Y., Yashar, B.M., Errede, B., Nishida, E., and Matsumoto, K. (1994). Stimulatory effects of yeast and mammalian 14–3-3 proteins on the Raf protein kinase. Science *265*, 1716–1719.

Ito, M., Iwase, M., Kodama, H., Lavisse, P., Komamine, A., Nishihama, R., Machida, Y., and Watanabe, A. (1998). A novel *cis*-acting element in promoters of plant B-type cyclin genes activates M phase-specific transcription. Plant Cell *10*, 331–341.

Ito, M., Araki, S., Matsunaga, S., Itoh, T., Nishihama, R., Machida, Y., Doonan, J.H., and Watanabe, A. (2001). G2/M-phase-specific transcription during the plant cell cycle is mediated by c-Myb-like transcription factors. Plant Cell *13*, 1891–1905.

Kakimoto, T., and Shibaoka, H. (1988). Cytoskeletal ultrastructure of phragmoplast-nuclei complexes isolated from cultured tobacco cells. Protoplasma (suppl.) *2*, 95–103.

Kishimoto, K., Matsumoto, K., and Ninomiya-Tsuji, J. (2000). TAK1 mitogen-activated protein kinase kinase kinase is activated by autophosphorylation within its activation loop. J. Biol. Chem. *275*, 7359–7364.

Krysan, P.J., Young, J.C., and Sussman, M.R. (1999). T-DNA as an insertional mutagen in *Arabidopsis*. Plant Cell *11*, 2283–2290.

Lee, K.S., Yuan, Y.L., Kuriyama, R., and Erikson, R.L. (1995). Plk is an M-phase-specific protein kinase and interacts with a kinesin-like protein, CHO1/MKLP-1. Mol. Cell. Biol. *15*, 7143–7151.

Lee, Y.-R., Giang, H.M., and Liu, B. (2001). A novel plant kinesin-related protein specifically associates with the phragmoplast organelles. Plant Cell *13*, 2427–2439.

Lloyd, C., and Hussey, P. (2001). Microtubule-associated proteins in plants—why we need a map. Nat Rev Mol Cell Biol. *2*, 40–47.

Lukowitz, W., Mayer, U., and Jürgens, G. (1996). Cytokinesis in the *Arabidopsis* embryo involves the syntaxin-related KNOLLE gene product. Cell *84*, 61–71.

Lupas, A., Van Dyke, M., and Stock, J. (1991). Predicting coiled coils from protein sequences. Science *252*, 1162–1164.

Miyajima, I., Nakafuku, M., Nakayama, N., Brenner, C., Miyajima, A., Kaibuchi, K., Arai, K., Kaziro, Y., and Matsumoto, K. (1987). *GPA1*, a haploid-specific essential gene, encodes a yeast homolog of mammalian G protein which may be involved in mating factor signal transduction. Cell *50*, 1011–1019.

Nagata, K., Puls, A., Futter, C., Aspenstrom, P., Schaefer, E., Nakata, T., Hirokawa, N., and Hall, A. (1998). The MAP kinase kinase kinase MLK2 colocalizes with activated JNK along microtubules and associates with kinesin superfamily motor KIF3. EMBO J. *17*, 149–158.

Nishihama, R., and Machida, Y. (2001). Expansion of the phragmoplast during plant cytokinesis: a MAPK pathway may MAP it out. Curr. Opin. Plant Biol. *4*, 507–512.

Nishihama, R., Banno, H., Kawahara, E., Irie, K., and Machida, Y. (1997). Possible involvement of differential splicing in regulation of the activity of *Arabidopsis* ANP1 that is related to mitogen-activated protein kinase kinase kinases (MAPKKKs). Plant J. *12*, 39–48.

Nishihama, R., Ishikawa, M., Araki, S., Soyano, T., Asada, T., and Machida, Y. (2001). The NPK1 mitogen-activated protein kinase kinase kinase is a regulator of cell-plate formation in plant cytokinesis. Genes Dev. *15*, 352–363.

Posas, F., and Saito, H. (1998). Activation of the yeast SSK2 MAP kinase kinase kinase by the SSK1 two-component response regulator. EMBO J. *17*, 1385–1394.

Raich, W.B., Moran, A.N., Rothman, J.H., and Hardin, J. (1998). Cytokinesis and midzone microtubule organization in *Caenorhabditis elegans* require the kinesin-like protein ZEN-4. Mol. Biol. Cell *9*, 2037–2049.

Sakurai, H., Miyoshi, H., Mizukami, J., and Sugita, T. (2000). Phosphorylation-dependent activation of TAK1 mitogen-activated protein kinase kinase kinase by TAB1. FEBS Lett. *474*, 141–145.

Samuels, A.L., Giddings, T.H., Jr., and Staehelin, L.A. (1995). Cytokinesis in tobacco BY-2 and root tip cells: a new model of cell plate formation in higher plants. J. Cell Biol. *130*, 1345–1357.

Semiarti, E., Ueno, Y., Tsukaya, H., Iwakawa, H., Machida, C., and Machida, Y. (2001). The *ASYMMETRIC LEAVES2* gene of *Arabidopsis thaliana* regulates formation of a symmetric lamina, establishment of venation and repression of meristem-related homeobox genes in leaves. Development *128*, 1771–1783.

Severson, A.F., Hamill, D.R., Carter, J.C., Schumacher, J., and Bowerman, B. (2000). The Aurora-related kinase AIR-2 recruits ZEN-4/CeMKLP1 to the mitotic spindle at metaphase and is required for cytokinesis. Curr. Biol. *10*, 1162–1171.

Shibuya, H., Yamaguchi, K., Shirakabe, K., Tonegawa, A., Gotoh, Y., Ueno, N., Irie, K., Nishida, E., and Matsumoto, K. (1996). TAB1: an activator of the TAK1 MAPKKK in TGF-β signal transduction. Science *272*, 1179–1182.

Staehelin, L.A., and Hepler, P.K. (1996). Cytokinesis in higher plants. Cell *84*, 821–824.

Stevenson, B.J., Rhodes, N., Errede, B., and Sprague, G.F., Jr. (1992). Constitutive mutants of the protein kinase STE11 activate the yeast pheromone response pathway in the absence of the G protein. Genes Dev. *6*, 1293–1304.

Strompen, G., El Kasmi, F., Richter, S., Lukowitz, W., Assaad, F.F., Jürgens, G., and Mayer, U. (2002). The *Arabidopsis HINKEL* gene encodes a kinesin-related protein involved in cytokinesis and is expressed in a cell cycle-dependent manner. Curr. Biol. *12*, 153–158.

Takekawa, M., and Saito, H. (1998). A family of stress-inducible GADD45-like proteins mediate activation of the stress-responsive MTK1/MEKK4 MAPKKK. Cell *95*, 521–530.

Tanaka, K., Matsumoto, K., and Toh-e, A. (1989). IRA1, an inhibitory regulator of the RAS-cyclic AMP pathway in *Saccharomyces cerevisiae*. Mol. Cell. Biol. *9*, 757–768.

Tanaka, H., Onouchi, H., Kondo, M., Hara-Nishimura, I., Nishimura, M., Machida, C., and Machida, Y. (2001). A subtilisin-like serine protease is required for epidermal surface formation in *Arabidopsis* embryos and juvenile plants. Development *128*, 4681–4689.

Tsuda, L., Inoue, Y.H., Yoo, M.A., Mizuno, M., Hata, M., Lim, Y.M., Adachi-Yamada, T., Ryo, H., Masamune, Y., and Nishida, Y. (1993). A protein kinase similar to MAP kinase activator acts downstream of the raf kinase in *Drosophila*. Cell *72*, 407–414.

Verhey, K.J., Meyer, D., Deehan, R., Blenis, J., Schnapp, B.J., Rapoport, T.A., and Margolis, B. (2001). Cargo of kinesin identified as JIP scaffolding proteins and associated signaling molecules. J. Cell Biol. *152*, 959–970.

Yasuhara, H., and Shibaoka, H. (2000). Inhibition of cell-plate formation by brefeldin A inhibited the depolymerization of microtubules in the central region of the phragmoplast. Plant Cell Physiol. *41*, 300–310.

Yasuhara, H., Sonobe, S., and Shibaoka, H. (1993). Effects of taxol on the development of the cell plate and of the phragmoplast in tobacco BY-2 cells. Plant Cell Physiol. *34*, 21–29.

Yen, T.J., Compton, D.A., Wise, D., Zinkowski, R.P., Brinkley, B.R., Earnshaw, W.C., and Cleveland, D.W. (1991). CENP-E, a novel human centromere-associated protein required for progression from metaphase to anaphase. EMBO J. *10*, 1245–1254.

Yen, T.J., Li, G., Schaar, B.T., Szilak, I., and Cleveland, D.W. (1992). CENP-E is a putative kinetochore motor that accumulates just before mitosis. Nature *359*, 536–539.

Zecevic, M., Catling, A.D., Eblen, S.T., Renzi, L., Hittle, J.C., Yen, T.J., Gorbsky, G.J., and Weber, M.J. (1998). Active MAP kinase in mitosis: localization at kinetochores and association with the motor protein CENP-E. J. Cell Biol. *142*, 1547–1558.

Zuo, J., Niu, Q.-W., Nishizawa, N., Wu, Y., Kost, B., and Chua, N.-H. (2000). KORRIGAN, an *Arabidopsis* endo-1,4-β-glucanase, localizes to the cell plate by polarized targeting and is essential for cytokinesis. Plant Cell *12*, 1137–1152.

Accession Numbers

Sequences of *NACK1*, *NACK2*, and AtNACK1 cDNAs have been deposited in GenBank under accession numbers AB071435, AB071436, and AB081599, respectively.